POLITECNICO DI TORINO
Repository ISTITUZIONALE

Assembly of Nano-Biocatalyst for the Tandem Hydrolysis and Reduction of p-Nitrophenol Esters

Original
Assembly of Nano-Biocatalyst for the Tandem Hydrolysis and Reduction of p-Nitrophenol Esters / RIBEIRO DE BARROS, Heloise; Yukari Tanaka, Lívia; Trivella Pacheco da Silva, Rafael; Santiago-Arcos, Javier; Córdoba de Torresi, Susana I.; López-Gallego, Fernando. - In: PARTICLE & PARTICLE SYSTEMS CHARACTERIZATION. - ISSN 0934-0866. - 38:10(2021). [10.1002/ppsc.202100136]

Availability:
This version is available at: 11583/2995218 since: 2024-12-12T09:53:33Z

Publisher:
John Wiley and Sons Inc

Published
DOI:10.1002/ppsc.202100136

Terms of use:

This article is made available under terms and conditions as specified in the corresponding bibliographic description in the repository

Publisher copyright
Wiley preprint/submitted version

This is the pre-peer reviewed version of the [above quoted article], which has been published in final form at http://dx.doi.org/10.1002/ppsc.202100136.This article may be used for non-commercial purposes in accordance with Wiley Terms and Conditions for Use of Self-Archived Versions..

(Article begins on next page)

06 May 2026

This is the pre-peer reviewed version of the following article: Barros, HR; Tanaka, LY; da Silva, RTP; Santiago-Arcos, J; Torresi, SIC; López-Gallego, F. Assembly of Nano-Biocatalyst for the Tandem Hydrolysis and Reduction of p-Nitrophenol Esters. Part. Part. Syst. Charact. 2021, 2100136, which has been published in final form at 10.1002/ppsc.202100136..

This article may be used for non-commercial purposes in accordance with Wiley Terms and Conditions for Use of Self-Archived Versions."

Assembly of nano-biocatalyst for the tandem hydrolysis and reduction of p-nitrophenol esters

Heloise Ribeiro de Barros, Lívia Yukari Tanaka, Rafael Trivella Pacheco da Silva, Javier Santiago-Arcos, Susana I. Córdoba de Torresi, and Fernando López-Gallego**

Dr. H.R. de Barros, L.Y. Tanaka, R.T.P. da Silva, Prof. S.I.C. de Torresi
Department of Fundamental Chemistry, Institute of Chemistry
University of São Paulo
Av. Prof. Lineu Prestes, 748, Vila Universitária, 05508-000 São Paulo, SP, Brazil
E-mail: barroshr@usp.br

Dr. H.R. de Barros, J. Santiago-Arcos, Prof. Dr. F. López-Gallego
CIC biomaGUNE, Basque Research and Technology Alliance (BRTA)
Paseo de Miramón 182, 20014 Donostia – San Sebastián, Spain.

Prof. F. López-Gallego
Ikerbasque, Basque Foundation for Science, 48013 Bilbao, Spain

Keywords: Biocatalysis, Chemo-enzymatic cascade reactions, Colloidal Chemistry, Interfacial interactions, Nanocatalysis, Nanostructures

Hybrid nano-biomaterials are exploited in the design and performance of chemo-enzymatic cascades. In this work, we immobilize lipase from *Candida antarctica* fraction B (CALB) and gold nanoparticles (Au NPs) on magnetic particles coated with silica (MNP@SiO_2) to stepwise hydrolyze and reduce p-nitrophenyl esters in tandem reaction. The assembly of the two catalysts at the interface of the MNP@SiO_2 particles and the temporal control of the reaction turns out to be the most determinant parameters for the cascade kinetics. When both CALB and Au NPs are co-immobilized at the MNP@SiO_2 particle, the tandem reactions take place significantly faster than when both catalysts are physically segregated by their immobilization on different MNP@SiO_2 particles. Herein, we demonstrate that the co-immobilization of biocatalysts and nanocatalysts in solid materials creates hybrid interfaces that accelerated chemo-enzymatic tandem reactions.

1. Introduction

Combining biocatalysis and nanocatalysis for chemo-enzymatic cascade reaction emerges as an excellent opportunity to design new reaction schemes. However, controlling the conditions that preserve the efficiency and compatibility of both catalysts under the same reaction conditions remains challenging.[1, 2] As an example, optimal reaction conditions (such as optimal temperature and pH-values) for each catalysts must be met towards a successful cascade reaction.[2] When catalysts incompatibility precludes the cascade process, either temporal or spatial segregation of the catalytic species is intended.[3] Using a homogeneous catalyst, the most common approach is the sequential addition of the chemical catalyst first, followed by the addition of the biocatalyst. However, a concurrent process in one-pot is sometimes unaffordable through this approach.[4] As an alternative, the immobilization of the catalysts allows their physical segregation, eases their separation, and enables their recycling.[5] When both catalysts poison each other due to molecular contacts, their anchoring to solid surfaces avoids such as poisoning allowing the cascade performance in a concurrent manner within the same reaction vessel. Moreover, the interfacial interactions can influence the microenvironment between the catalysts, which may impact the diffusion and reaction rates of the cascade reactions.[6] Therefore, understanding the interfacial interactions that take place between bio- and metal-catalysts is of fundamental importance to overcome the challenges of the intrinsic complexity of cascade reactions involving nano-biocatalysts.[2, 7]

Metallic nanoparticles, often employed as metallic nanocatalysts, are lastly successfully combined with biocatalysts to route chemo-enzymatic cascades. One example that illustrates the potential of this approach is the conjugation of the lipase from *Candida antarctica* fraction B (CALB) on metallic NPs towards the use in cascade reactions.[8-10] Bionanohybrids of CALB–Pd NPs[9] and self-assemblies composed of CALB–Cu NPs[10] exemplify the hydrolysis of 4-nitrophenyl butyrate (biocatalysis) followed by the reduction of the product 4-nitrophenol (metal catalysis) in a sequential chemo-enzymatic reactions.

Besides the catalytic synergy between enzymes and the metallic NPs, the latter can also be used as carriers to immobilize enzymes with the aim at enhancing the activity, stability, and operational performance of the immobilized enzymes.[11, 12] For example, enzyme immobilization on magnetic NPs eases the biocatalyst recovery and reuse under magnetic fields.[11, 13] The activity of enzymes immobilized on quantum dots and gold NPs were significantly enhanced when compared to the free enzymes and it was influenced by the size of the respective NPs.[12] Although the examples cited above illustrate the synergy between NPs and enzymes, the role of the spatial organization of the catalysts in the cascade performance is barely known.

In this study, we investigate different assemblies of CALB and gold nanoparticles (Au NPs) immobilized on solid support materials to maximize the efficiency of a model chemo-enzymatic cascade that converts p-nitrophenyl esters into p-aminophenol. Magnetic particles coated with a thin silica shell (MNP@SiO_2) were used as artificial support to control the localization of both Au NPs and CALB. The support materials with magnetic properties ease their separation and re-use.[14] Furthermore, the silica shell provides a versatile surface to be functionalized and is biocompatible for enzyme immobilization.[15, 16] As results, we synthesized

heterogeneous nano-biocatalysts based on Au NPs and CALB immobilized on MNP@SiO_2 assembled in different manners. Finally, we tested these hybrid nano-biocatalysts for the model chemo-enzymatic cascade reaction to study whether the overall cascade kinetics are affected by the localization of both catalysts.

2. Results and Discussion

Before performing the model chemo-enzymatic cascade, we firstly designed a preparation route (**Scheme 1**) to fabricate a hybrid heterogeneous catalyst that harbors CALB and Au NPs on the surface of MNP@SiO_2. First, we obtained hollow MNPs with diameters of 218 ± 17 nm (**Figure 1A and S1**) that were further coated with SiO_2 to avoid oxidation and aggregation of the particles (**Figure 1B**). As a result, a silica layer of ~ 15 nm was formed on the surface of the MNPs (**Figure 1B**, **inset**). The MNP@SiO_2 were further functionalized with 3-aminopropyltriethoxysilane (APTES) to introduce terminal amine groups on the material. Those positively charged amines were used to interact with negatively charged Au NPs (~12 nm) previously prepared by citrate reduction following standard protocols (see methods) to fabricate MNP@SiO_2-Au. **Figure 1C** shows that Au NPs were uniformly distributed on the MNP@SiO_2 structure. Lastly, CALB was immobilized on the surface of the MNP@SiO_2-Au,

forming a thin organic layer all over the material structure presumably correspondent to the adsorbed enzyme (**Figure 1D**).

When we intended altering the immobilization order and CALB was firstly conjugated to the surface of the Au NPs and that complex was subsequently immobilized on the MNP@SiO_2, the enzyme activity was reduced to 12% (**Table S1**). Conversely, the direct adsorption of CALB on the MNP@SiO_2 allowed us to recover roughly 50% of the enzyme activity upon the immobilization process. With this result in hands and together with the TEM images, we suggest that CALB is immobilized on the

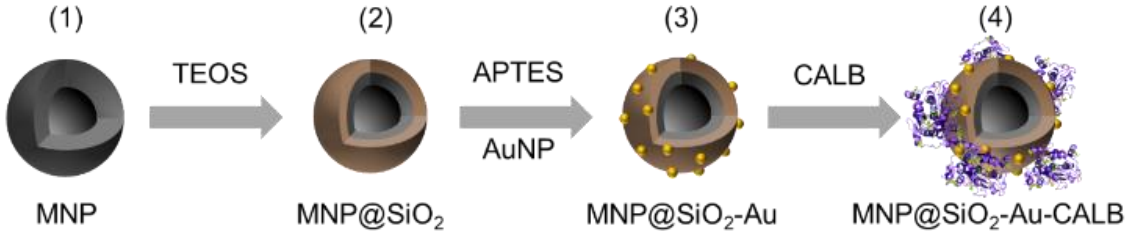

Scheme 1. Illustrative representation of the subsequent steps in the synthesis of the hybrid nano-biocatalyst MNP@SiO_2-Au-CALB. (1) Hollow MNPs were coated with (2) a layer of SiO_2, which was modified with APTES for further functionalization of (3) Au NPs. Lastly, (4) CALB was conjugated on the surface of the material to obtain the final material MNP@SiO_2-Au-CALB. Graphic representation not drawn to scale.

functionalized SiO_2 shell rather than on the Au NPs, although the minor role of the direct interaction of CALB with the gold surface may not be discarded because of the known binding affinity between biomolecules and Au NPs[17].

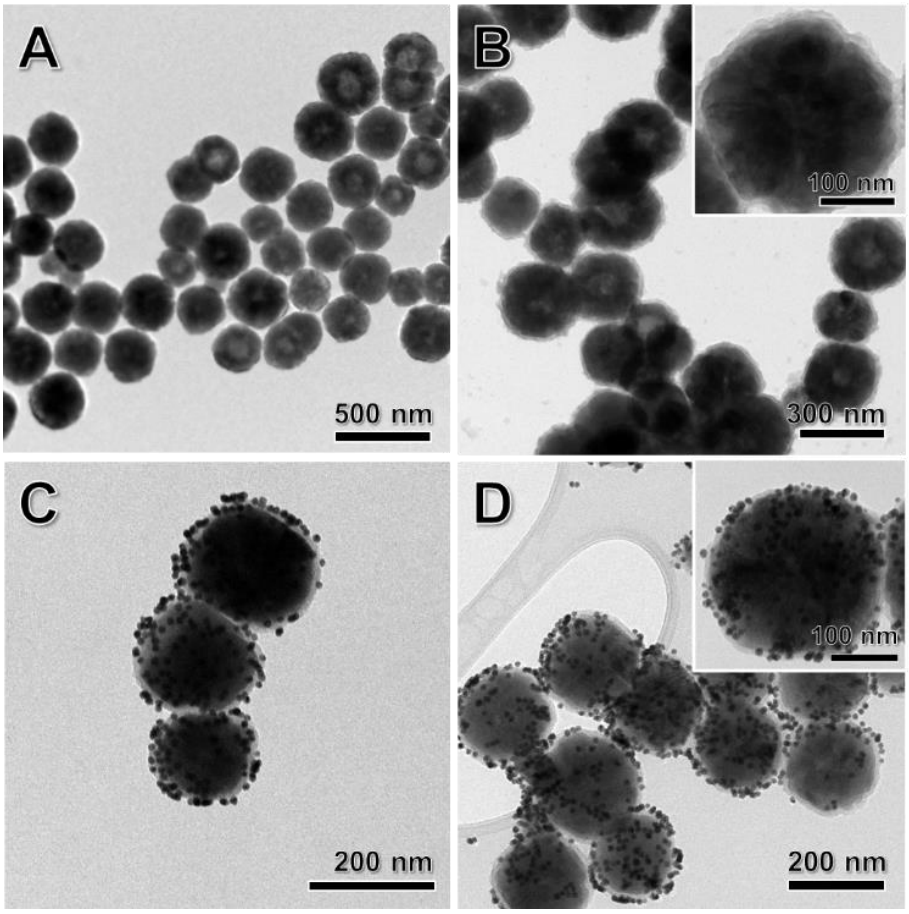

Figure 1. TEM images of the (A) hollow MNP as-prepared, (B) coated with a layer of SiO_2 (MNP@SiO_2), (C) further functionalized with the Au NPs (MNP@SiO_2-Au), and the (D) final structure coated by CALB (MNP@SiO_2-Au-CALB). Insets of the images evidenced the silica shell (B) and the functionalization of Au NPs and CALB (D) on the surface of the MNP@SiO_2.

The cascade reaction takes place through the hydrolysis of p-nitrophenyl palmitate (*p*NPP) to p-nitrophenolate (*p*NP) (CALB mediated), followed by the reduction of *p*NP to p-aminophenol (*p*AP) (Au NPs mediated) in the presence of an excess of $NaBH_4$ as the reducing agent (see **Scheme 2**). Previous X-ray photon spectroscopy (XPS) studies revealed that the energy binding of Au NPs supported on SiO_2 particles is correspondent to Au^0 species,[22] which supports that we have metallic Au in our systems (as also observed by the TEM images). The gold in this oxidation

state is well known to be ready to catalyze the reduction of p-nitrophenol in presence of sodium borohydride.

We selected both *p*NPP hydrolysis and *p*NP reduction as they are model reactions very often explored in biocatalysis and nanocatalysis, respectively.[18-21] Before analyzing the chemo-enzymatic cascade reactions, we first analyzed individually each reaction catalyzed by the hybrid nano-biocatalyst. The reaction rate per mass of the hybrid nano-biocatalyst were independently determined for the enzyme hydrolysis (V_0 = 90.7 μM min^{-1} per mg of MNP@SiO_2) and for the AuNP driven nitroreduction (specific apparent rate constant (k_{app}) = 0.018 min^{-1}) (**Figure S1**). Similar performance was observed for CALB immobilized on Cu NPs towards chemo-enzymatic cascade reaction with p-nitrophenol esters.[10] In addition, CALB remained active for at least 22 days, presenting similar activity over the time for CALB immobilized on either MNP@SiO_2 and MNP@SiO_2-Au as well as free CALB. Therefore, the kinetic constants demonstrated that both CALB and Au NPs at the hybrid nano-biocatalyst are active and can work independently.

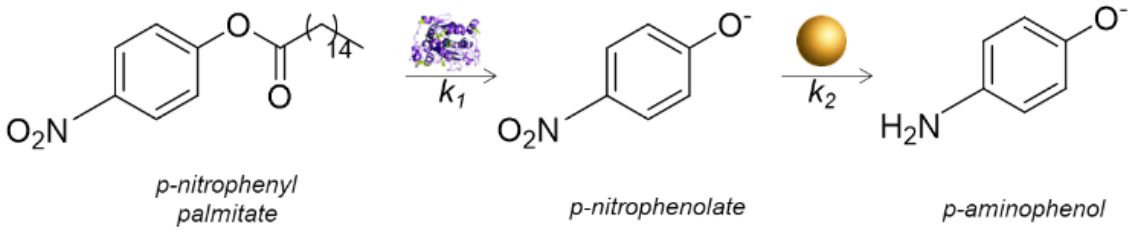

Scheme 2. Cascade reaction catalyzed by the hybrid nano-biocatalyst: *p*NPP hydrolysis biocatalyzed by CALB, releasing *p*NP as a product (k_1), which is subsequently reduced to *p*AP via nanocatalysis by Au NPs (k_2) in presence of $NaBH_4$.

Notably, the catalytic properties of CALB were not affected by the excess of $NaBH_4$ used for the *p*NP reduction in the cascade reactions. The hydrolysis of the *p*NPP in the presence or absence of $NaBH_4$ showed fairly similar performance **(Figure S2A**),

confirming that $NaBH_4$ negligibly affects the CALB catalytic activity. Moreover, even though the excess of $NaBH_4$ led to the increase of pH solution from 7.4 to 9, this consequence did not hamper the enzyme activity either. Indeed, the increase of pH itself was not able to trigger *p*NPP hydrolysis in the absence of CALB (**Figure 2A**). Moreover, the reduction of the *p*NP did not take place in absence of the Au NPs, revealing that Au NPs are needed for the reduction of the *p*NP as expected **(Figure 2B**). Hence, both proposed cascade reactions only proceeded when both CALB and Au NPs were presented in the same reaction media.

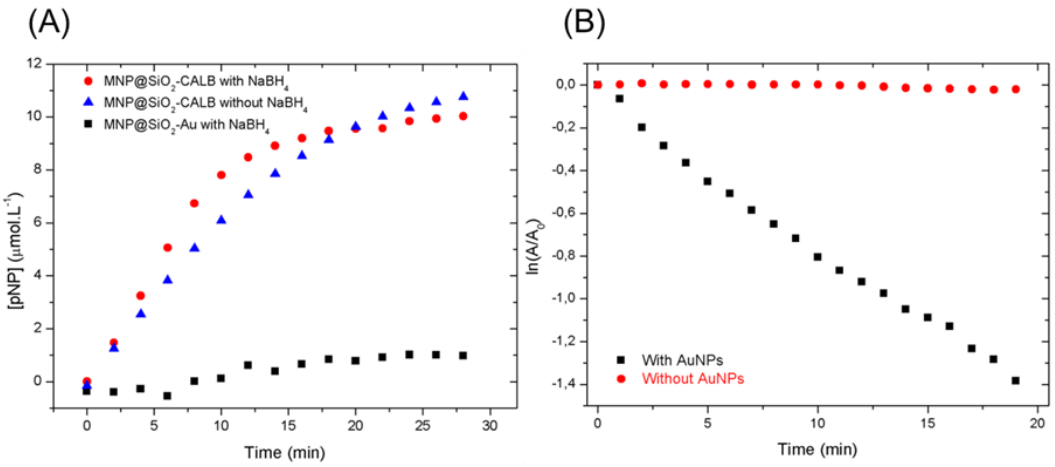

Figure 2. (A) Time-courses of *p*NPP hydrolysis catalyzed by MNP@SiO_2-CALB in presence (red data) and absence (blue data) of excess of $NaBH_4$, and by MNP@SiO_2-Au in absence of CALB (black squares). (B) Plot of $\ln(A/A_o)$ as a function of time for *p*NP reduction in presence of $NaBH_4$ as a reducing agent with (black data) and without (red data) Au NPs.

Once demonstrated that both catalysts selectively perform their corresponding reactions, we performed the chemo-enzymatic cascade in two different modes: 1) sequential cascade where $NaBH_4$ was added after the *p*NPP hydrolysis step was completed (**Scheme 3A and C**) concurrent cascade where both *p*NPP and $NaBH_4$ substrates were added to the reaction mixture from the beginning (time 0) (**Scheme 3B and D**). These two reaction modes were carried out with the hybrid nano-biocatalysts assembled in different manners. In one case, CALB and AuNPs were co-immobilized

on the same support material (MNP@SiO_2-Au-CALB) (**Scheme 3A and B**). On the other, CALB and AuNPs were immobilized on different supports (MNP@SiO_2-Au and MNP@SiO_2-CALB) and then mixed in the reaction bulk (**Scheme 3C and D**). While in the first case, both the enzyme and the nanocatalyst are closely in contact at the nanoscale facilitating the diffusion of the intermediates between the two catalytic centers (**Scheme 3B**), in the second configuration they are physically segregated forcing the intermediates to diffuse from one catalyst to the other through the reaction bulk (**Scheme 3D**).

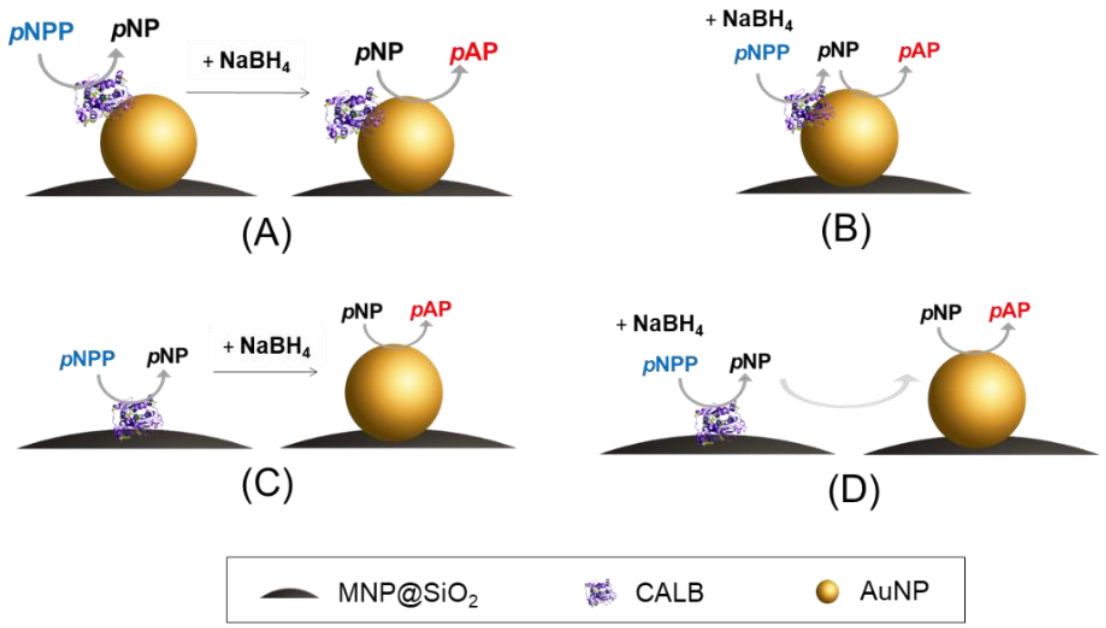

Scheme 3. Schematic illustration of the chemo-enzymatic cascade reaction catalyzed by CALB and Au NPs when co-immobilized (MNP@SiO_2-Au-CALB) (A and B) or physically segregated on the MNP@SiO_2 support (MNP@SiO_2-Au and MNP@SiO_2-CALB) (C and D) performed in the sequential (A and C) and concurrent (B and D) reaction modes. Graphic representation not drawn to scale.

Using a hybrid nano-biocatalyst where CALB and AuNPs co-immobilized on the silica surface and a sequential reaction mode (**Scheme 3A**), the concentration of the *p*NP increased rapidly until reaching a plateau (approx. 40 min), which meant the quantitative hydrolysis of *p*NPP (**Figure 3A, red**). Upon addition of $NaBH_4$, the *p*NP

was abruptly but not quantitatively reduced to *p*AP as approx. 10% of *p*NP remained unreacted. In contrast, in the concurrent approach where the reaction is triggered by adding both *p*NPP and $NaBH_4$ (**Scheme 3B**), the *p*NP intermediated was accumulated during the first 5 min of reaction (**Figure 3B, red**) and then decayed presumably by the reduction of *p*NP to *p*AP. After 60 minutes of concurrent reaction, 3.8 μM of *p*NP remained unreacted. This behavior suggests that the second step (*p*NP reduction) was

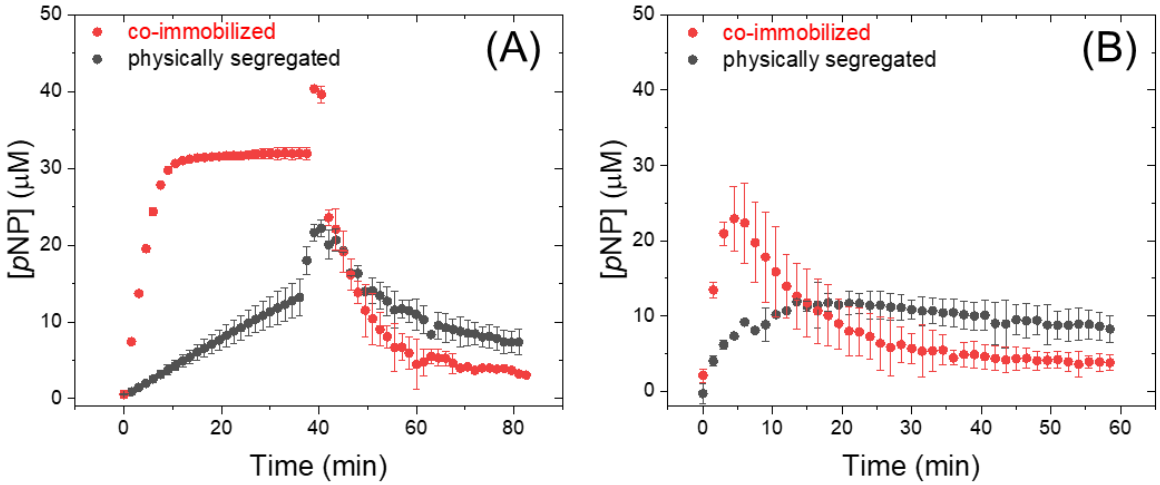

Figure 3. Monitoring of *p*NP concentration as a function of time in the chemo-enzymatic cascade reaction as (A) sequential and (B) concurrent modes catalyzed by the hybrid nano-biocatalyst, in which CALB and AuNPs were co-immobilized (MNP@SiO_2-Au-CALB) (red) or physically segregated (MNP@SiO_2-Au and MNP@SiO_2-CALB) (black) on the MNP@SiO_2 support.

triggered before the first step (*p*NPP hydrolysis) was fully completed. However, the second step was uncompleted (approx. 90% conversion) as the intermediate can still be detected. The levels of the unreacted intermediate in the bulk were similar in both concurrent and sequential chemo-enzymatic reaction modes, likely to the complete hydrolysis of the $NaBH_4$ after 60 min of reaction.

On the contrary, the reaction kinetics were significantly reduced for both sequential and concurrent cascades catalyzed by the CALB and Au NPs physically segregated in different MNP@SiO_2 (**Scheme 3C and D**). The segregated configuration

enables the hydrolysis of the *p*NPP at the surface of MNP@SiO_2-CALB but the produced *p*NP molecules must diffuse from such particles to those decorated with Au NPs (MNP@SiO_2-Au) to yield the final product *p*AP. For the sequential approach, only 54% of *p*NPP was enzymatically hydrolyzed, yielding roughly 13.2 μM of *p*NP that was further reduced to *p*AP by the supported AuNPs but with a limited conversion of 44% according to the 7.4 μM unreacted *p*NP detected upon the cascade completion (**Figure 3A, black**). Interestingly, the segregated system reduced *p*NP slower than the co-immobilized hybrid nano-biocatalyst working sequentially under the same reaction conditions. Finally, when the segregated hybrid nano-biocatalyst was applied in the concurrent chemo-enzymatic cascade, we observed the worst results in terms of kinetics and intermediate accumulation. After 10 minutes, 10 μM of *p*NP was accumulated but it was poorly reduced to yield the final product (**Figure 3B, black**).

To better understand the kinetics of the chemo-enzymatic process, we firstly determined the V_0 and k_{app} of the hybrid nano-biocatalyts for each reaction step using the time courses of the sequential mode shown in **Figure 3A**. The hydrolysis V_0 of the co-immobilized hybrid nano-biocatalyst was 10 times higher than its physically segregate counterpart (**Table 1**). Therefore, the co-immobilization of CALB with Au NPs at the surface of MNP@SiO_2 enhances the enzyme efficiency. Next, we estimated the k_{app} for the second cascade step. By plotting $\ln([p\text{NP}]_t/[p\text{NP}]_{t=0})$ *vs* time, we find that the gold-mediated *p*NP can be described as a pseudo-first-order rate law[20] (**see Figure S3**). A similar rate law was proposed for the reduction of ferrocyanate III catalyzed by colloidal Au NPs using $NaBH_4$ as a reducing agent.[23] As expected from the time courses of the sequential cascade, the k_{app} of the co-immobilized system MNP@SiO_2-Au-CALB was 368% higher than the physically segregated MNP@SiO_2-Au and MNP@SiO_2-CALB catalysts.

Table 1. Kinetic parameters determined from the sequential cascade reactions catalyzed by the hybrid nano-biocatalyst when co-immobilized (MNP@SiO_2-Au-CALB) or physically segregated on the MNP@SiO_2 support (MNP@SiO_2-Au and MNP@SiO_2-CALB).[a)]

Nano-biocatalyst	Sequential	
	V_0 ($\mu M\ min^{-1}$)	k_{app} ($10^{-2}\ min^{-1}$)
MNP@SiO_2-Au-CALB[b)]	3.4 ± 0.3	8.9 ± 0.4
MNP@SiO_2-Au and MNP@SiO_2-CALB [c)]	0.35 ± 0.01	2.42 ± 0.1

[a)] Reaction conditions: PBS Buffer pH 7.4 at room temperature (~ 25°C); [b)] Enzyme concentration = 5.4 μM, Au concentration = 0.2 mM; [c)] Enzyme concentration = 5.0 μM, Au concentration = 0.2 mM.

To confirm that the kinetics reported in **Table 1** for the sequential system were still valid for the concurrent cascade, we proposed a two-reaction kinetic model presented in **Scheme 4**, in which k_1 is the first-order constant of the hydrolysis reaction defined as V_o/[CALB] and k_2 is the first-order constant of the reduction reaction defined as k_{app}. Using the software COPASI[24] and the kinetic parameters reported in **Table 1**, we modelled the performance of both co-immobilized and physically segregated hybrid nano-biocatalysts for the concurrent hydrolysis/nitroreduction of *p*NPP into *p*AP. **Figure 4** shows the simulated accumulation of *p*NP compared to the experimental data. We observed that the model was less accurate to predict the intermediate accumulation in the physically segregated system, likely due to the fact that transport of the intermediate from one catalyst to the next was not considered in the model. To demonstrate that the transport of *p*NP was affecting the efficiency of the process, we

Scheme 4. Cascade reaction catalyzed by the hybrid nano-biocatalyst in the sequential system: *p*NPP hydrolysis biocatalyzed by CALB, releasing *p*NP as a product (k_1), followed by the additional transport rate between CALB and Au NPs (k_t), and subsequently reduced to *p*AP via nanocatalysis by Au NPs (k_2) in presence of $NaBH_4$.

created a second kinetic model including an additional transport constant k_t that defines the transport rate between the CALB and the Au NPs:

We found that using the arbitrary value of k_t = 0.1 min^{-1}, the model fitted much better to the experimental data, supporting the hypothesis that the segregated systems was kinetically limited by the *p*NP transport between the two catalysts.

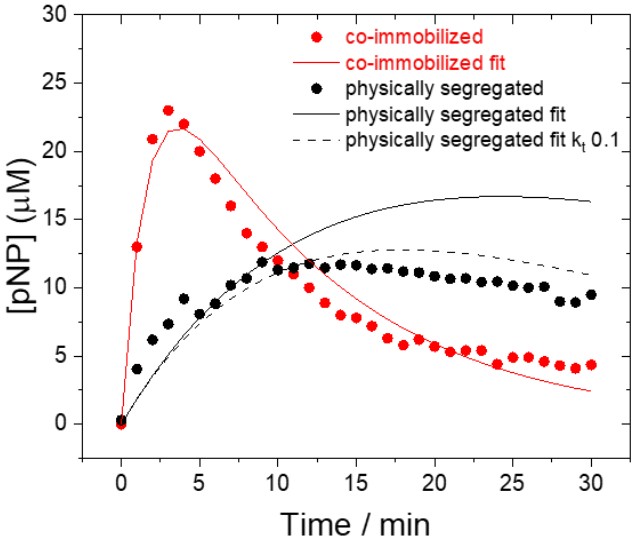

Figure 4. Fitting (lines) of experimental (circles) chemo-enzymatic cascade reaction performed for the co-immobilized (red) and physically segregated (black) hybrid nano-biocatalysts. Data fitting were analyzed by COPASI software based on the reaction model presented in **Scheme 4**.

3. Conclusion

This study unveils that the physical proximity of CALB and Au NP co-immobilized on the surface of MNP@SiO_2 particles increases the efficiency of chemo-enzymatic cascade and minimizes the accumulation of the *p*NP intermediate. However, when CALB was directly bound to the surface of AuNP immobilized on MNP@SiO_2, the enzyme dramatically lost its activity. Experimental and modelling data support the importance of the assembly of the catalytic elements in the design of this type of hybrid nano-biocatalyst. Therefore, both CALB and AuNP must be close enough, but not directly interacting, to efficiently hydrolyze *p*NPP to *p*NP and facilitate the diffusion of

such intermediate from the catalytic site of CALB to the surface of the Au NPs. Hence, the co-immobilization of CALB and Au NPs across the surface of MNP@SiO_2 forms a "nanoreactor"[25] able to perform a concurrent model chemo-enzymatic cascade in one-pot. The physical proximity of both enzyme and nanoparticle enhances the overall performance of such a cascade. In the light of the evidence presented in this study, we suggest that the interplay of enzymes and nanoparticles at the interfaces with larger solid materials benefit their cooperative action.

4. Experimental Section/Methods

Materials

Iron (III) chloride hexahydrate ($FeCl_3.6H_2O$), ethylene glycol, ammonium hydroxide, toluene, and ethanol were purchased from Synth. Sodium hydroxide, sodium citrate tribasic dehydrate, polyvinyl pyrolidone (PVP MW 40.000), (3-aminopropyl) triethoxysilane (APTES), tetrachloroauric (III) acid ($HAuCl_4$), tetraethyl orthosilicate (TEOS), phosphate buffered saline (PBS) pH 7.4, lipase from *Candida antarctica* fraction B (CALB), 4-nitrophenyl palmitate (*p*NPP), and sodium borohydride ($NaBH_4$) were purchased from Sigma-Aldrich.

Hybrid nano-biomaterial synthesis

MNP synthesis

In a previously described procedure[26], 1.35 g of $FeCl_3.6H_2O$ and 0.7g of NaOH were dissolved in 60 mL of ethylene glycol and kept under vigorous magnetic stirring for two hours. Ultrasonic bath was used in the meantime to facilitate dissolution. The final solution was transferred to a 100 mL Teflon-line stainless autoclave and kept at 200°C for 40 hours. After cooling the solution down to room temperature, the precipitate was separated with a neodymium magnet and washed twice with ethanol, three times with water and resuspended in ethanol to dry in an oven at 80°C.

MNP@SiO_2 synthesis

In a sol-gel procedure[15], two solutions named A and B were prepared. In solution A, 5g of PVP were dissolved in 55 mL of distilled water and kept under magnetic stirring until complete dissolution. Solution B was composed by 100 mg of Fe_3O_4 suspended in 15 mL of distilled water and stirred with an overhead stirrer. Ultrasonic bath was used in the meantime to facilitate dissolution in both solutions. Solution A was added to the solution B flask, where the final solution was stirred for 2 hours. Then, the supernatant was removed and a solution of 100 mL of ethanol and 5 mL of ammonium hydroxide was added followed by a solution of 1 mL of TEOS and 2 mL of ethanol. The final solution was stirred for two hours. The resultant solid was separated with a neodymium magnet and washed twice with ethanol, three times with water and resuspended in ethanol to dry in an oven at 80°C.

MNP@SiO_2-Au synthesis

62.5 mg of MNP@SiO_2 previously prepared were dissolved in 9.38 mL of dry toluene and kept in ultrasonic bath for 30 minutes[15]. Then, 93.8 μL of APTES were added dropwise under constant stirring for 2 hours. The precipitate was collected with a neodymium magnet and washed once with toluene and twice with acetone and dried in an oven at 80°C. Then, 100 mg of the amino-functionalized MNP@SiO_2 were added to 150 mL of AuNPs colloidal suspension. AuNPs were previous obtained by the typical Turkevich method[27], in which 100 mg of sodium citrate dissolved in 150 mL of distilled water was heated to boiling before adding 1 mL of $HAuCl_4$ 25 mmol.L^{-1}, and further kept under magnetic stirring at 100°C for 15 minutes. Finally, the resulting material MNP@SiO_2-Au was kept in ultrasonic bath for 30 minutes and overhead stirred for one hour. The precipitate was collected using a neodymium magnet, washed several times with ethanol and distilled water and dried in an oven at 80°C.

MNP@SiO_2-Au-CALB synthesis

A 0.1 mg.mL^{-1} of CALB solution was prepared in PBS buffer at pH 7.4. Another solution of 0.1 mg.mL^{-1} of MNP@SiO_2-Au (or MNP@SiO_2) was prepared in PBS buffer at pH 7.4. Then, solutions with a ratio 1:1 of CALB and MNP@SiO_2-Au (or MNP@SiO_2) were kept under overhead stirrer for two hours. The final solid was recovered with a neodymium magnet and washed with PBS. The washed solid was resuspended in PBS resulting in a final concentration of 0.25 mg.mL^{-1} of the material, whose contain 0.18 mg.mL^{-1} of protein. The final material was kept at 4°C to avoid CALB denaturation.

Electron microscopy characterization

The MNPs were characterized by scanning electron microscopy (SEM) using a FESEM JEOL JSM-7401F at an acceleration voltage of 5.0 kV in the Chemistry Institute at São Paulo University. Samples were prepared by dropping approx. 10 mL on the silicon wafers and left to dry. The hybrid nano-biomaterials were characterized by transmission electron microscopy (TEM) using a JEOL JEM-1400PLUS microscope at an acceleration voltage of 120 kV. Samples were prepared by dropping approx. 3 mL on the carbon-coated copper grids and left to dry.

Catalytic activity assays

pNPP hydrolysis

The enzymatic activity was determined by the hydrolysis of *p*NPP, monitoring the release of *p*NP using a UV-Vis spectroscopy at λ = 405 nm.[19] 120 μL of the substrate *p*NPP (0.5 mM) previously prepared in isopropanol was added in a quartz cuvette containing 1.83 mL of PBS buffer and 150 μL of the sample to be determined. The molar extinction coefficient of ε = 13000 L.mol^{-1}.cm^{-1} was used to determine the *p*NP concentration.[28]

pNP reduction

The catalytic activity of the Au NPs was determined by *p*NP reduction to *p*AP, monitoring its consumption using a UV-Vis spectroscopy at λ = 405 nm.[20, 21] In a quartz cuvette containing 1.83 mL of PBS buffer, 60 mL of *p*NP 0.5 mmol.L^{-1}, and 150 mL of the samples to be analyzed, was added 50 µL of a 38 mg.mL^{-1} $NaBH_4$ solution. The molar extinction coefficient of ε = 13000 L.mol^{-1}.cm^{-1} was used to determine the *p*NP concentration.[28]

Sequential cascade reaction

The sequential cascade reaction proceeded in two steps. The first one is the hydrolysis of *p*NPP to *p*NP. In a quartz cuvette, 1.83 mL of PBS were added with 120 µL of the substrate *p*NPP (0.5 mM) and 150 µL of the MNP@SiO_2-Au-CALB (0.25 mg.mL^{-1}). When MNP@SiO_2-Au and MNP@SiO_2-CALB were studied in separate, 150 µL of each catalyst (0.25 mg.mL^{-1}) were added . The reaction was monitored by UV-Vis spectra at 405 nm until a plateau was reached. Next, the second step consisted in the *p*NP reduction to *p*AP through the addition of 50 µL of a 38 mg.mL^{-1} of $NaBH_4$. The second part of the reaction was monitored by UV-Vis spectra at 405 nm to monitor the *p*NP consumption. The reactions were assessed using a Shimadzu UV-2600 UV-Vis spectrophotometer.

Concurrent cascade reaction

The concurrent cascade reaction proceeded in a single step. Both hydrolysis of *p*NPP and reduction of *p*NP occurred simultaneously. Therefore, the reducing agent $NaBH_4$ was added at the same step of the other components. In a quartz cuvette, 1.83 mL of PBS were added with 120 µL of *p*NPP (0.5 mM), 50 µL of a 38 mg.mL^{-1} $NaBH_4$ solution, and 150 µL of the MNP@SiO_2-Au-CALB. When MNP@SiO_2-Au and MNP@SiO_2-CALB were studied in separate, 150 µL of each catalyst were added

instead. The reaction was monitored by UV-Vis spectra at 405 nm using a Shimadzu UV-2600 UV-Vis spectrophotometer.

Supporting Information
Supporting Information is available from the Wiley Online Library or from the author.

Acknowledgements
The authors thank Brazilian agencies CNPq and São Paulo Research Foundation FAPESP (2015/26308-7 and 2018/13492-2) for financial support. H.R.B. also thanks FAPESP for the fellowships granted (2019/09668-0 and 2017/20892-4). L.Y.T. also thanks FAPESP for the fellowships granted (2019/19551-3 and 2018/02435-8). R.T.P.S. acknowledges CAPES for the fellowship (88882.328241/2019-01). J.S-A thanks the PhD fellowship (PRE2019-090835) funded by the Spanish State Research Agency. F.L-G thanks IKERBASQUE for the funding. This This work was performed under the Maria de Maeztu Units of Excellence Program from the Spanish State Research Agency – Grant No. MDM-2017-0720. We also sincerely thank Prof. Luis M. Liz-Marzán for kindly providing his laboratory for the kinetic experiments.

Received: ((will be filled in by the editorial staff))
Revised: ((will be filled in by the editorial staff))
Published online: ((will be filled in by the editorial staff))

References

[1] D. J. Mikolajczak, B. Koksch, *Chemcatchem* **2018**, *10*, 4324-4328; C. A. Denard, J. F. Hartwig, H. M. Zhao, *Acs Catalysis* **2013**, *3*, 2856-2864.
[2] S. Schmidt, K. Castiglione, R. Kourist, *Chemistry-a European Journal* **2018**, *24*, 1755-+.
[3] Y. Liu, P. Liu, S. Gao, Z. Wang, P. Luan, J. González-Sabín, Y. Jiang, *Chemical Engineering Journal* **2020**.
[4] N. Rios-Lombardia, C. Vidal, M. Cocina, F. Moris, J. Garcia-Alvarez, J. Gonzalez-Sabin, *Chemical Communications* **2015**, *51*, 10937-10940.
[5] D. P. Debecker, V. Smeets, M. Van der Verren, H. M. Arango, M. Kinnaer, F. Devred, *Current Opinion in Green and Sustainable Chemistry* **2021**, *28*, 1-6; T. Gorbe, K. P. J. Gustafson, O. Verho, G. Kervefors, H. Q. Zheng, X. D. Zou, E. V. Johnston, J. E. Backvall, *Acs Catalysis* **2017**, *7*, 1601-1605; K. P. J. Gustafson, T. Gorbe, G. De Gonzalo, N. Yuan, C. L. Schreiber, A. Shchukarev, C. W. Tai, I. Persson, X. D. Zou, J. E. Backvall, *Chemistry-a European Journal* **2019**, *25*, 9174-9179.
[6] M. Pavlovic, A. Plucinski, J. R. Zhang, M. Antonietti, L. Zeininger, B. Schmidt, *Langmuir* **2020**, *36*, 1401-1408; A. Kuchler, M. Yoshimoto, S. Luginbuhl, F. Mavelli, P. Walde, *Nature Nanotechnology* **2016**, *11*, 409-420.
[7] C. Schmidt-Dannert, F. Lopez-Gallego, *Microbial Biotechnology* **2016**, *9*, 601-609.

[8] C. M. Kisukuri, D. J. Palmeira, T. S. Rodrigues, P. H. C. Camargo, L. H. Andrade, *Chemcatchem* **2016**, *8*, 171-179.
[9] M. Filice, M. Marciello, M. D. Morales, J. M. Palomo, *Chemical Communications* **2013**, *49*, 6876-6878.
[10] Z. X. Li, Y. Ding, X. L. Wu, J. Ge, P. K. Ouyang, Z. Liu, *Rsc Advances* **2016**, *6*, 20772-20776.
[11] S. A. Ansari, Q. Husain, *Biotechnology Advances* **2012**, *30*, 512-523.
[12] J. C. Breger, E. Oh, K. Susumu, W. P. Klein, S. A. Walper, M. G. Ancona, I. L. Medintz, *Bioconjugate Chemistry* **2019**, *30*, 2060-2074; J. C. Breger, M. G. Ancona, S. A. Walper, E. Oh, K. Susumu, M. H. Stewart, J. R. Deschamps, I. L. Medintz, *Acs Nano* **2015**, *9*, 8491-8503.
[13] M. Sarno, M. Iuliano, *Applied Surface Science* **2019**, *474*, 135-146.
[14] H. Vaghari, H. Jafarizadeh-Malmiri, M. Mohammadlou, A. Berenjian, N. Anarjan, N. Jafari, S. Nasiri, *Biotechnology Letters* **2016**, *38*, 223-233; M. C. M. de Souza, K. P. dos Santos, R. M. Freire, A. C. H. Barreto, P. B. A. Fechine, L. R. B. Goncalves, *Brazilian Journal of Chemical Engineering* **2017**, *34*, 681-690.
[15] M. Abbas, S. R. Torati, C. S. Lee, C. Rinaldi, C. Kim, *Journal of Nanomedicine & Nanotechnology* **2014**, *5*, 244.
[16] A. G. Roca, D. Carmona, N. Miguel-Sancho, O. Bomati-Miguel, F. Balas, C. Piquer, J. Santamaria, *Nanotechnology* **2012**, *23*.
[17] J. Mosquera, I. Garcia, M. Henriksen-Lacey, M. Martinez-Calvo, M. Dhanjani, J. L. Mascarenas, L. M. Liz-Marzan, *Acs Nano* **2020**, *14*, 5382-5391; R. Garcia-Alvarez, M. Hadjidemetriou, A. Sanchez-Iglesias, L. M. Liz-Marzan, K. Kostarelos, *Nanoscale* **2018**, *10*, 1256-1264; M. S. J. Sajib, P. Sarker, Y. Wei, X. P. Tao, T. Wei, *Langmuir* **2020**, *36*, 13356-13363.
[18] K. E. Jaeger, B. W. Dijkstra, M. T. Reetz, *Annual Review of Microbiology* **1999**, *53*, 315-+; M. L. Li, G. F. Chen, *Nanoscale* **2013**, *5*, 11919-11927; R. D. Neal, Y. Inoue, R. A. Hughes, S. Neretina, *Journal of Physical Chemistry C* **2019**, *123*, 12894-12901.
[19] C. S. Wu, C. T. Wu, Y. S. Yang, F. H. Ko, *Chemical Communications* **2008**, 5327-5329; H. R. d. Barros, I. García, C. Kuttner, N. Zeballos, P. H. C. Camargo, S. I. Cordoba de Torresi, F. López-Gallego, L. M. Liz-Marzán, *ACS Catalysis* **2020**, *Submitted*.
[20] P. Herves, M. Perez-Lorenzo, L. M. Liz-Marzan, J. Dzubiella, Y. Lu, M. Ballauff, *Chemical Society Reviews* **2012**, *41*, 5577-5587.
[21] E. C. M. Barbosa, J. L. Fiorio, T. Mou, B. Wang, L. M. Rossi, P. H. C. Camargo, *Chemistry-a European Journal* **2018**, *24*, 12330-12339.
[22] J. J. Luo, W. Chu, S. Sall, C. Petit, *Colloids and Surfaces a-Physicochemical and Engineering Aspects* **2013**, *425*, 83-91; T. Herranz, X. Y. Deng, A. Cabot, Z. Liu, M. Salmeron, *Journal of Catalysis* **2011**, *283*, 119-123.
[23] S. Carregal-Romero, J. Perez-Juste, P. Herves, L. M. Liz-Marzan, P. Mulvaney, *Langmuir* **2010**, *26*, 1271-1277.
[24] S. Hoops, S. Sahle, R. Gauges, C. Lee, J. Pahle, N. Simus, M. Singhal, L. Xu, P. Mendes, U. Kummer, *Bioinformatics* **2006**, *22*, 3067-3074.
[25] H. C. Zeng, *Chemcatchem* **2020**, *12*, 5303-5311; R. Kamarudheen, G. Kumari, A. Baldi, *Nature Communications* **2020**, *11*.
[26] Y. Zong, H. N. Xin, J. R. Zhang, X. H. Li, J. Feng, X. Deng, Y. Sun, X. L. Zheng, *Journal of Magnetism and Magnetic Materials* **2017**, *423*, 321-326.
[27] J. Turkevich, P. C. Stevenson, J. Hillier, *Discussions of the Faraday Society* **1951**, 55-&.

[28] A. I. Biggs, *Transactions of the Faraday Society* **1954**, *50*, 800-802.

The assembly of biocatalysts and nanocatalysts matters to the more efficient chemo-enzymatic cascade reactions. The comparison of co-immobilized and physically segregated assemblies revealed that interfacial interactions played a key role in both concurrent and sequential nano-biocatalysis reaction modes. The overall performance was regulated by exploiting the localization of enzymes and Au nanoparticles on the surface of magnetic nanoparticles.

H. R. de Barros,* L. Y. Tanaka, R. T. P. da Silva, J. Santiago-Arcos, S. I. C. de Torresi, and F. López-Gallego*C.

Assembly of nano-biocatalyst for the tandem hydrolysis and reduction of p-nitrophenol esters

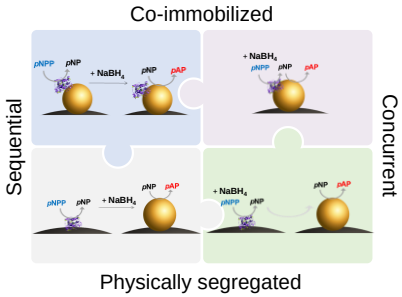

Supporting Information

Assembly of nano-biocatalyst for the tandem hydrolysis and reduction of p-nitrophenol esters

Heloise Ribeiro de Barros, Lívia Yukari Tanaka, Rafael Trivella Pacheco da Silva, Javier Santiago-Arcos, Susana I. Córdoba de Torresi, and Fernando López-Gallego**

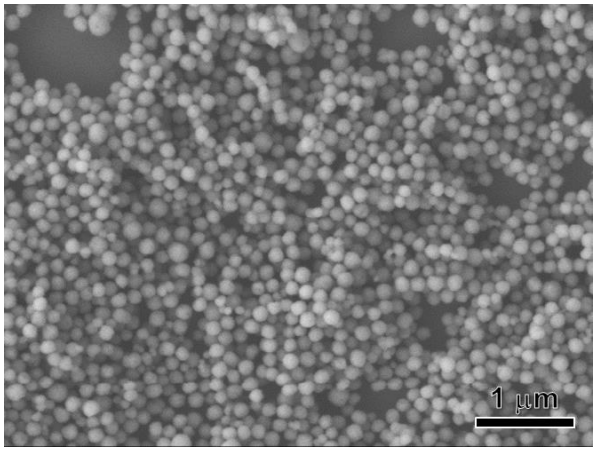

Figure S1. SEM image of the as-prepared MNPs.

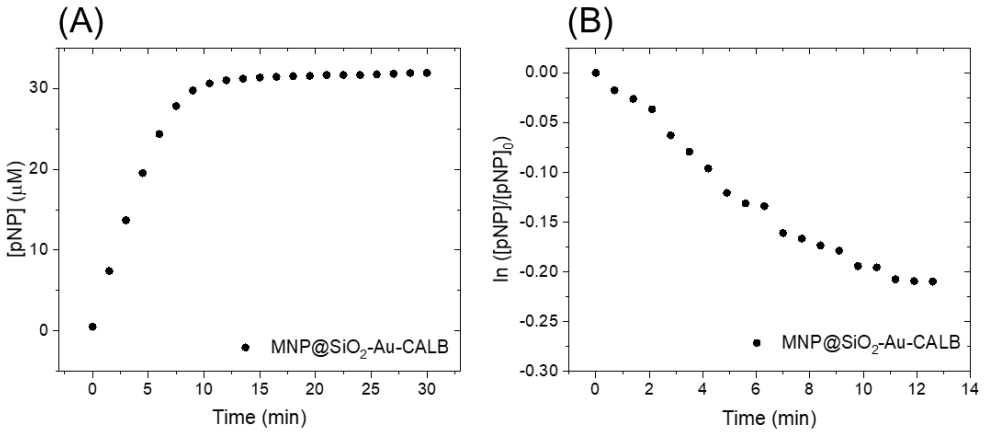

Figure S2. Time-courses of (A) *p*NPP hydrolysis and (B) *p*NP reduction reactions catalyzed by MNP@SiO_2-Au-CALB.

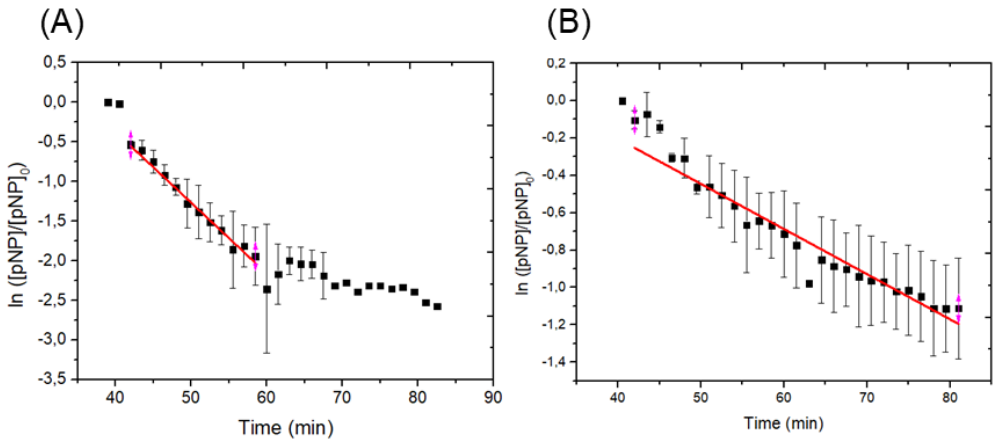

Figure S3. Plot of ln([*p*NP]$_t$/[*p*NP]$_{t=0}$) as a function of time for *p*NP reduction by the (A) co-immobilized (MNP@SiO_2-Au-CALB) and the (B) physically segregated (MNP@SiO_2-Au and MNP@SiO_2-CALB) systems performed in the sequential cascade reaction.

Table S1. Enzyme activity and enzyme loading of the catalysts.

Sample	Expressed activity (%)	Immobilization yield (%)
[a] MNP@SiO_2-CALB	55	11
[b] MNP@SiO_2-Au-CALB	46	13
[c] AuNP@CALB/MNP@SiO_2	12	16

[a] CALB immobilized on the MNP@SiO_2; [b] Au NPs functionalized on the MNP@SiO_2, further adsorption of CALB; [c] CALB immobilized on Au NPs, further immobilized on the MNP@SiO_2.